

Passive matching of large nonlinear phase in ultrafast twin-core fiber amplifier for coherent combination

HUAIQIN LIN¹, YUJUN FENG^{1,*}, PRANABESH BARUA^{1, 2}, W. MINSTER KUNKEL³, JONATHAN H. V. PRICE¹, JAYANTA SAHU¹, JAMES R. LEGER³, AND JOHAN NILSSON¹

¹*Optoelectronics Research Centre, University of Southampton, Southampton SO17 1BJ, UK*

²*Present address SPI Lasers UK Ltd, Tollbar Way, 6 Wellington Park, Hedge End, Southampton SO30 2QU*

³*Department of Electrical and Computer Engineering, University of Minnesota, 200 Union street SE, Minneapolis, MN 55455, USA*

*Corresponding author: Yujun.Feng@soton.ac.uk

Received XX October 2020; revised XX Month, XXXX; accepted XX Month XXXX; posted XX Month XXXX (Doc. ID XXXXX); published XX Month XXXX

We use a bespoke design and fabrication procedure to realize a polarization-maintaining Yb-doped fiber with two near-identical, un-coupled, cores, suitable for coherent beam combination (CBC) of ultrashort pulses at large nonlinear phase accumulation. Using an in-house Dammann grating for seeding the two cores from a common input, we experimentally evaluated parabolic-pulse amplification at 1064 nm. From a measured output interference pattern at a *B*-integral of 26 rad \pm 15% according to simulations, we calculated a theoretical CBC efficiency of 88.5%, which to our knowledge is unprecedented with such high nonlinear phase. This suggests an averaged difference in *B* between channels of at most 0.5 rad (1.9% of 26 rad). Also, the 27 nm spectral width requires better than 17 μ m optical path-length (OPL) matching. The OPL and *B*-integral remained stably equalized as *B* increased to 26 rad, suggesting that multi-core fibers with carefully fabricated cores are well suited to power and energy scaling through CBC of pulses at high nonlinearity. © 2020 Optical Society of America

OCIS codes: (060.2320) *Fiber optics amplifiers and oscillators*; (140.3510) *Lasers, fiber*; (120.5050) *Phase measurement*.

<http://dx.doi.org/10.1364/OL.99.099999>

Coherent beam combination (CBC) of ultrafast pulses amplified in parallel fiber amplifiers has seen considerable progress in recent years [1-7]. First and foremost, CBC requires that the beams be mutually coherent with controlled relative phase. Furthermore, the optical pathlength (OPL) of the channels must be equal to within a fraction of the (length-equivalent) transform-limited pulse duration, e.g., with differential delay with active feedback to compensate for thermal and other slow drifts. These affect the phase, too, which needs control to within a small fraction of 2π , typically with kHz-level bandwidth.

During a pulse, there are also much faster nonlinear phase

effects (“nonlinear phase”) related to the instantaneous power (self-phase modulation, SPM, quantified by the *B*-integral) [8, 9], as well as weaker effects related to extracted energy (Kramers Kronig’s effect and instantaneous heating) [10, 11]. This can differ between channels, and varies too quickly for intra-pulse feedback control. Thus, any difference between channels must be kept much below 2π through other means. This is challenging at large nonlinear phase. If *B* = 25 rad, the difference between amplifiers must lie within 2% to enable a phase error < 0.5 rad and thus a CBC efficiency $\eta > 90\%$ [8]. Not only high peak power but also high pulse energy, e.g., as targeted with divided-pulse amplification [9, 10, 12-14], can cause significant phase differences between unequal channels [11].

Several experiments on ultrafast pulse combination have demonstrated good efficiency at relatively large *B*. For example, two pulses to be combined can counter-propagate through the same amplifier, so that their nonlinear-phase envelopes are nearly the same even without active control. In a femtosecond fiber chirped-pulse amplification (CPA) system, $\eta = 84\%$ was achieved at *B* = 12 rad [1] and 91.5% at 7 rad [3]. To the best of our knowledge, the highest reported *B*-integral is 12 rad in a system with active phase stabilization, with $\eta = 89\%$ [2]. Another experiment combined four femtosecond Yb-doped fiber (YDF) amplifiers to 3.5 kW of average power with $\eta = 88.2\%$ at *B* = 11 rad [7]. In such parallel configurations, the pump or seed power can be adjusted channel-wise to minimize the phase difference [15], but with pulses, this cannot equalize the phase in every instance, e.g., if gain saturation at high pulse energy distorts the shape. A more general way for ns pulses (e.g., in CPA) is to control the intra-pulse phase profile with electro-optic phase modulators [16], but this requires an expensive modulator in each channel and cannot reduce any channel-dependent response to pulse-to-pulse fluctuations [17].

Simultaneously, fibers with multiple un-coupled cores are investigated for ultrafast CBC. This has been demonstrated with four [18], seven [5, 19], 12 [4], 16 [6], and 49 [20] cores at *B* < 8 rad. Attractions include increased commonality in phase

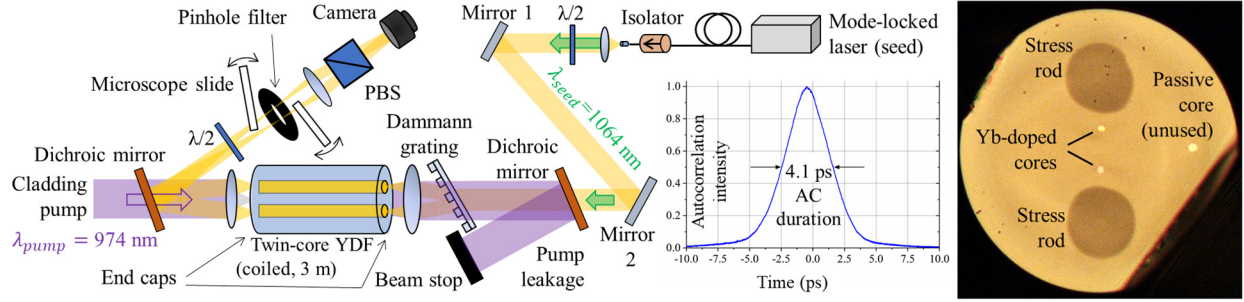


Fig. 1. Schematic of the amplifier with twin-core YDF, beam combination and measurement setup. An autocorrelation trace of the seed pulses is also shown, together with a facet image of the twin-core YDF, formed by light launched into its opposite end. The YDF is circular but chipped in the image.

fluctuations, fewer parts, and compactness. For higher energy and peak power, ultrafast CBC in multicore fibers at higher B are of great interest.

In this paper, we demonstrate amplification in the ultrafast parabolic-pulse regime in a polarization-maintaining (PM) twin-core YDF in a two-channel master oscillator – power amplifier (MOPA). This is seeded by 3-ps pulses centered at 1064 nm, which are divided into two beams matched to the two un-coupled cores by a Dammann grating, designed and fabricated in-house. We measured the visibility of interfered amplified pulses, and calculated theoretically a CBC efficiency of nearly 90%, when B was 26 rad according to simulations and the linewidth was 27 nm. Then, CBC is highly sensitive to OPD and relative difference in B . During the experiments, we took no steps to equalize B . Furthermore, the linear phase was stable over several seconds and changes in the OPD were negligible. We attribute the high visibility and stability to the YDF, which we designed and fabricated with a procedure that reduces differences in properties, pumping, and temperature between the cores.

Figure 1 shows the MOPA and visibility measurement setup, and a facet image of the 3-m PM twin-core double-clad YDF used for the amplifier. White light was launched into the YDF's opposite end, and a silicon-array camera imaged the facet with transmitted light. We attribute intensity contrasts to the refractive index rather than to absorption. The Yb doped core diameter is $\sim 3.4 \mu\text{m}$ and the numerical aperture (NA) is 0.24, so $V = 2.4$ at 1064 nm. Each core operated cleanly on a single spatial mode. The core centers are $\sim 21 \mu\text{m}$ apart, which provides a similar thermal environment and still avoids optical coupling. The cores sit between $\sim 38\text{-}\mu\text{m}$ -diameter rods, which are boron-doped to induce stress and thus birefringence in the cores. Each core center is $\sim 9 \mu\text{m}$ from the edge of its closer rod. The intensity in Fig. 1 is lower in the stress rods because boron lowers the refractive index. The inner cladding is circular with $153 \mu\text{m}$ diameter, and is coated by a low-index polymer. An ancillary passive core of $\sim 4.3\text{-}\mu\text{m}$ diameter was not used in these experiments. The stress rods break the circular geometry, which improves the pump absorption.

Whereas a typical PM fiber has its core in the middle of two stress-applying parts (e.g., rods) [21], our design has each core much closer to one stress rod than the other. Then, the stress originates largely from the close rod. According to COMSOL calculations, the birefringence becomes 41% of what it would be if the remote stress rod is moved to the same distance from the core as the closer stress rod. Though the 59%-reduction is significant, substantial birefringence remains. Furthermore, the birefringence with the present arrangement is larger than if the cores are placed

symmetrically on the other, orthogonal, line of symmetry, if the stress rods remain in the same location.

In Fig. 1, the YDF was loosely coiled in four $\sim 20\text{-cm}$ -diameter loops and taped to the optical table. Both ends were spliced to end-caps comprising 400- μm -diameter coreless fiber, and had normal output facets. The amplifier was seeded by a mode-locked fiber source (Fianium FemtoPower 1060-2-FS), which generates linearly polarized, 50-MHz repetition rate pulses centered at 1064 nm. The autocorrelation (AC) duration was measured to $\sim 470\text{-fs}$ (full-width at half maximum, FWHM) at full power ($\sim 2 \text{ W}$). At other power levels, the pulses are longer and chirped. We set the seed laser to generate positively chirped pulses (bandwidth $\sim 11 \text{ nm}$) of 100 mW of average power. The measured AC duration was 4.1 ps (inset, Fig. 1), from which the pulse duration was evaluated to $\sim 3.5 \text{ ps}$. Throughout this paper, we quote FWHM durations, where pulse durations are determined by fitting split-step simulations of the nonlinear Schrödinger equation in RP Fiber Power [22] to measured AC durations. For this, we used the demonstration file "Parabolic pulses in Yb amplifier.fpw" with appropriate parameters.

The seed pulses were collimated and coupled into the cores through a series of mirrors, a Dammann grating [23] designed and fabricated in-house, and a lens. A half-wave plate aligned the polarization with a principal axis of the cores. The Dammann grating converts a normally-incident beam into two beams corresponding to the $\pm 1^{\text{st}}$ grating orders with a theoretical efficiency of 81%. The required π rad phase step of the rectangular-wave-shaped relief structure was precision-etched into a fused silica substrate. The pitch of our grating was chosen so that a subsequent lens focused these two diffraction orders into the YDF's cores. Small grating tilts precisely adjusted the apparent grating pitch for best match to the core spacing. The principle and operation of the Dammann grating are fully explained in Ref. [24].

Each core was seeded with an estimated 10 mW of power. Most of the remaining $\sim 80\text{-mW}$ of seed power propagated through the inner cladding with negligible gain. The YDF was counter-directionally cladding-pumped by a 974-nm diode laser (IPG PLD-10). A dichroic mirror (DM) separated the pump and pulse paths at each YDF end. The pump leakage was $\sim 60\%$.

An aspheric lens focused the incident pump beam into the YDF. It also reimaged the fiber facet, loosely focused onto an elliptical pinhole placed in the pulse beam path. This transmitted output pulses emerging from the cores,

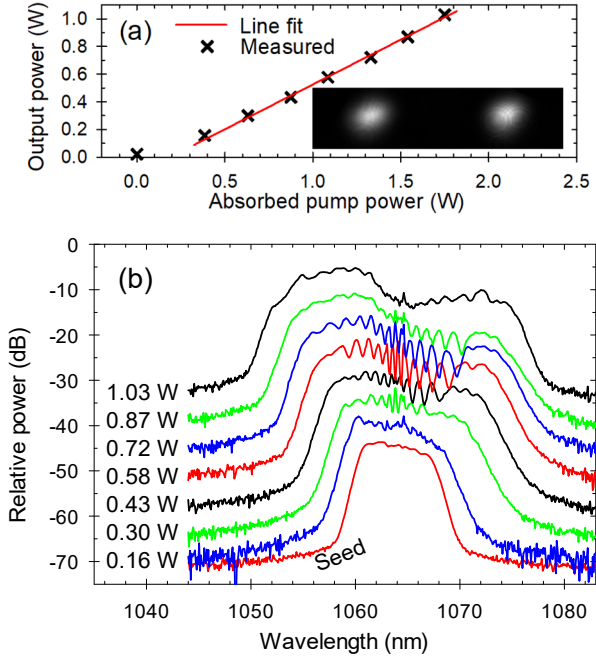


Fig. 2. (a) Pulse output power vs. pump power. Inset: Image of the two core output beams. (b) Spectra of output pulses (vertically offset for clarity) at output powers as indicated. Resolution 0.05 nm.

but blocked most cladding-guided light, comprising (amplified) spontaneous emission and a small amount of pulse light. In addition, a polarization beam splitter rejected light not in the pulses' dominant polarization. A half-wave plate before the pinhole minimized the rejection down to $\sim 2.5\%$ (-16 dB). A 300-mm focal-length lens spatially overlapped the two beams to form interference fringes on a silicon-array camera (Thorlabs DCC1545M). For approximate OPL equalization, each beam passed through a different microscope slide. One slide was angled to tune the OPL for its beam so that the fringe visibility was maximized. No retuning was needed as long as the setup was not perturbed. We also measured the intensity across the camera and power for each beam. They were balanced to within a few percent.

To evaluate the achievable combination efficiency, we first calculate the interference fringe visibility $V = (I_{\max} - I_{\min}) / (I_{\max} + I_{\min})$, where I_{\max} and I_{\min} are the maximum and minimum intensities along the central cross-section through the fringes. The degree of mutual coherence γ can be evaluated according to $|\gamma| = V(r_A + r_A^{-1})/2$, where $r_A = (I_1/I_2)^{1/2}$ and I_1 and I_2 are the intensities of the two beams [25]. Finally, the achievable combining efficiency becomes $\eta = (r_A + r_A^{-1} + 2|\gamma|) / (r_A^{1/2} + r_A^{-1/2})^2$. This assumes that the CBC compensates for any intensity differences. Thus, $\eta = 1$ if $|\gamma| = 1$ even if $I_1 \neq I_2$. For these, we further assume $I_1 = I_2$, whereby $V = |\gamma|$ and $\eta = (1+|\gamma|)/2 = (1+V)/2 = I_{\max} / (I_{\max} + I_{\min})$. This underestimates η if I_1 and I_2 are not optimally balanced.

We next describe the achieved amplification and visibility. The total pulse output power vs. absorbed pump power is shown in Fig. 2 (a). The output power increases linearly up to a maximum output power of 1.03 W for a gain of 17 dB, relative to the combined power launched into the cores. Images of the two output beams are shown, too. Fig. 2 (b) shows output pulse spectra. These broaden with increasing power because of SPM, and oscillations appear. The 20-dB bandwidth was ~ 11 nm without pumping and ~ 27 nm at full power. The output pulse duration increases to ~ 5.4 ps (6-ps AC)

without pumping, and to ~ 6.6 ps (8-ps AC) at full power.

Fig. 3 (a) plots B vs. absorbed pump power. Throughout this paper, the B -integral is not measured but determined from simulations of the power evolution and nonlinear broadening in RP Fiber Power. We obtained good agreement with measured quantities and estimate the uncertainty in the calculated B -integral to $\pm 15\%$. We neglected energy-related phase effects, because of the small pulse energy. The simulations also revealed a nonlinear coefficient $\gamma_{NL} = 2\pi n_2 / (\lambda A_{eff})$ of 10 rad kW $^{-1}$ m $^{-1}$. The visibility and combining efficiency as retrieved and calculated from interference patterns are plotted vs. B in Fig. 3 (b). They are highest at $B = 8$ rad, with $V = 0.93$ and $\eta = 96.5\%$. At $B = 26$ rad, they drop to $V = 0.77$ and $\eta = 88.5\%$. The reduction may be caused by differences in nonlinear phase and/or OPL between the cores. At large B , even small pulse fluctuations, e.g., from unstable launch, and differences between the cores can induce a significant difference in B . An RMS phase error of 0.49 rad (1.9% of 26 rad) is enough to degrade the CBC efficiency from 100% to 88.5% [26]. In addition, a broader spectrum reduces the visibility in the presence of OPD. The 27-nm linewidth at full power corresponds to ~ 56 fs (16 waves) of transform-limited pulse duration and thus to 17- μ m of OPL. This sets a limit on the OPD.

Fig. 4 plots the scaled intensity along the central cross section of the fringe pattern (shown in inset) at highest visibility (~ 0.93) and lowest visibility (i.e., at full power). The fringe positions were stable over several seconds, so also the linear phase was highly stable. The Gaussian-like envelope of the beam profile affected the visibility evaluation by at most $\sim 1\%$.

The two output beams are brought together, but are not parallel, so cannot be considered combined. Nevertheless, the conceptually simple addition of a combining element would realize CBC through beam stacking [27]. Alternatively, the two beams exiting the fiber could be individually collimated by separate micro-lenses to realize tiled CBC with the high fill factor required for high Strehl ratio [26]. We also note that in principle, the output beams at the fiber facet constitute two co-directional tiled beams, although with fill factor too small for practical CBC.

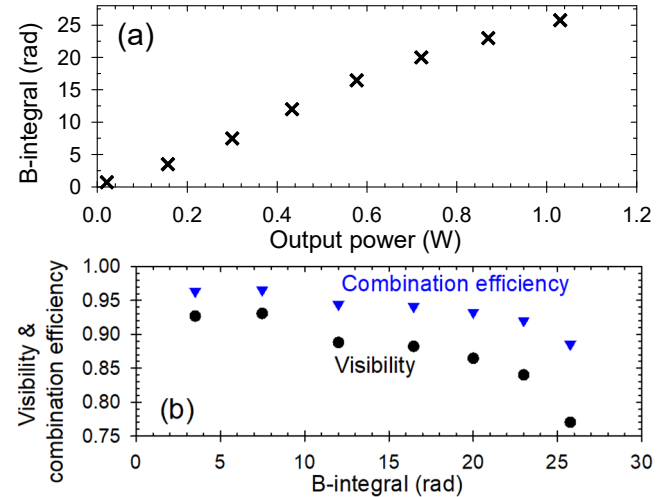


Fig. 3. (a) B -integral vs. pulse output power and (b) visibility and combining efficiency as evaluated from measured fringe pattern vs. B .

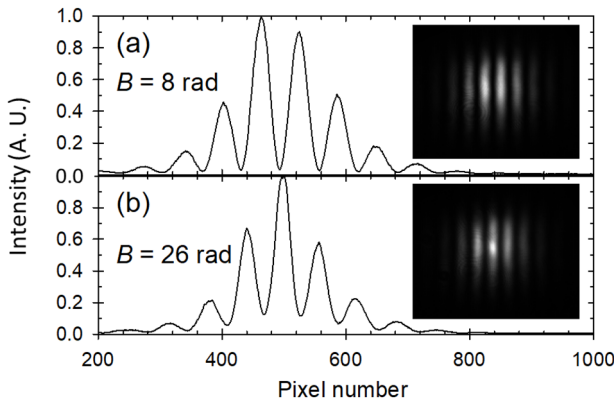


Fig. 4. Intensity distributions along the central cross section of the combined beam profile at (a) $B = 8$ rad and (b) $B = 26$ rad. Inset: measured interference pattern in the overlapped beam profiles.

To conclude, we have designed and fabricated a PM twin-core Yb-doped fiber for coherent beam combination of ultrashort pulses at large nonlinear phase. We experimentally evaluated parabolic-pulse amplification at 1064 nm at a B -integral as high as 26 rad, which is substantially larger than state-of-the-art values of around 10 rad in CBC demonstrations. From measurements of the visibility, we calculated a theoretical CBC efficiency of 88.5%, which suggests an averaged difference in phase between channels of at most 0.49 rad (1.9% of 26 rad). The spectral width reached 27 nm, and the OPD must be smaller than the transform-limited pulse length of ~ 17 μ m. Both nonlinear phase and OPL remained stably equalized as B increased up to 26 rad. The linear phase was also stable over several seconds. The thermal load was too low for appreciable thermo-optic effects, but we expect the OPD to remain small also at high thermal load, since thermal OPL changes are largely common for both cores. We did not study aging, but note that the nonlinear response is modified by photodarkening [11], which is expected to be similar in the two cores. Our results point to the possibility for CBC of ultrafast pulses at high nonlinearity with compact multicore fibers, with only the same level of phase control as used for narrow-line continuous-wave CBC, and without active OPD control.

Funding. Air Force Office of Scientific Research (FA9550-14-1-0382), Engineering and Physical Science Research Council (EP/P030181/1, EP/P027644/1, EP/P012248/1). H. Lin was financially supported by the China Scholarship Council.

Acknowledgement. We thank Dr Rüdiger Paschotta for valuable discussions and help with RP Fiber Power.

Disclosures. The authors declare no conflicts of interest

REFERENCES

1. L. Danialt, M. Hanna, D. N. Papadopoulos, Y. Zaouter, E. Mottay, F. Druon, and P. Georges, Opt. Lett. **36**, 4023 (2011).
2. A. Klenke, E. Seise, S. Demmler, J. Rothhardt, S. Breitkopf, J. Limpert, and A. Tünnermann, Opt. Express **19**, 24280 (2011).
3. Y. Zaouter, L. Danialt, M. Hanna, D. N. Papadopoulos, F. Morin, C. Hönninger, F. Druon, E. Mottay, and P. Georges, Opt. Lett. **37**, 1460 (2012).
4. P. Rigaud, V. Kermene, G. Bouwmans, L. Bigot, A. Desfarges-Berthelemot, D. Labat, A. Le Rouge, T. Mansuryan, and A. Barthélémy, Opt. Express **21**, 13555 (2013).
5. L. P. Ramirez, M. Hanna, G. Bouwmans, H. E. Hamzaoui, M. Bouazaoui, D. Labat, K. Delplace, J. Pouysegur, F. Guichard, P. Rigaud, V. Kermene, A. Desfarges-Berthelemot, A. Barthélémy, F. Prévost, L. Lombard, Y. Zaouter, F. Druon, and P. Georges, Opt. Express **23**, 5406 (2015).
6. A. Klenke, M. Müller, H. Stark, F. Stutzki, C. Hupel, T. Schreiber, A. Tünnermann, and J. Limpert, Opt. Lett. **43**, 1519 (2018).
7. M. Müller, A. Klenke, A. Steinkopff, H. Stark, A. Tünnermann, and J. Limpert, Opt. Lett. **43**, 6037 (2018).
8. S. Jiang, M. Hanna, F. Druon, and P. Georges, Opt. Lett. **35**, 1293 (2010).
9. M. Kienel, A. Klenke, T. Eidam, M. Baumgartl, C. Jauregui, J. Limpert, and A. Tünnermann, Opt. Express **21**, 29031 (2013).
10. F. Guichard, L. Lavenu, M. Hanna, Y. Zaouter, and P. Georges, Opt. Express **24**, 25329 (2016).
11. Y. Feng, B. M. Zhang, and J. Nilsson, J. Lightwave Technol. **36**, 5521 (2018).
12. S. Zhou, F. W. Wise, and D. G. Ouzounov, Opt. Lett. **32**, 871 (2007).
13. Y. Zaouter, F. Guichard, L. Danialt, M. Hanna, F. Morin, C. Hönninger, E. Mottay, F. Druon, and P. Georges, Opt. Lett. **38**, 106 (2013).
14. T. Zhou, J. Ruppe, C. Zhu, I. Hu, J. Nees, and A. Galvanauskas, Opt. Express **23**, 7442 (2015).
15. H. Tünnermann, Y. Feng, J. Neumann, D. Kracht, and P. Weßels, Opt. Lett. **37**, 1202 (2012).
16. H. Lin, Y. Feng, J. H. V. Price, T. W. Hawkins, L. Dong, and J. Nilsson, in Laser Congress 2019 (ASSL, LAC, LS&C), OSA Technical Digest (Optical Society of America, 2019), paper ATH2A.2.
17. H. Lin, Y. Feng, J. H. V. Price, and J. Nilsson, IEEE Photonics Technol. Lett. **31**, 1662 (2019).
18. A. Klenke, M. Wojdyr, M. Müller, M. Kienel, T. Eidam, H. Otto, F. Stutzki, F. Jansen, J. Limpert, and A. Tünnermann, in 2015 European Conference on Lasers and Electro-Optics/European Quantum Electronics Conference (Optical Society of America, 2015), paper CJ_1_2.
19. I. Hartl, A. Marcinkevičius, H. A. McKay, L. Dong, and M. E. Fermann, in Advanced Solid-State Photonics (Optical Society of America, 2009), TuA6.
20. J. Lhermite, E. Suran, V. Kermene, F. Louradour, A. Desfarges-Berthelemot, and A. Barthélémy, Opt. Express **18**, 4783 (2010).
21. J. Noda, K. Okamoto, and Y. Sasaki, J. Lightwave Technol. **4**, 1071 (1986).
22. RP Fiber Power v. 7, www.rp-photonics.com/fiberpower.html.
23. H. Dammann and E. Klotz, Opt. Acta **24**, 505 (1977).
24. W. M. Kunkel and J. R. Leger, Opt. Express **26**, 9373 (2018).
25. G. R. Fowles, *Introduction to Modern Optics*, 2nd ed. (Dover Publications, 1989), p. 67.
26. J. R. Leger, in *Surface emitting semiconductor lasers and arrays*, G. Evans and J. Hammer, ed. (Academic Press, 1993), Ch. 8.
27. J. R. Leger, G. J. Swanson, and W. B. Veldkamp, Appl. Opt. **26**, 4391 (1987).

Full References

1. L. Daniault, M. Hanna, D. N. Papadopoulos, Y. Zaouter, E. Mottay, F. Druon, and P. Georges, "Passive coherent beam combining of two femtosecond fiber chirped-pulse amplifiers," *Opt. Lett.* **36**, 4023-4025 (2011).
2. A. Klenke, E. Seise, S. Demmler, J. Rothhardt, S. Breitkopf, J. Limpert, and A. Tünnermann, "Coherently-combined two channel femtosecond fiber CPA system producing 3 mJ pulse energy," *Opt. Express* **19**, 24280-24285 (2011).
3. Y. Zaouter, L. Daniault, M. Hanna, D. N. Papadopoulos, F. Morin, C. Hönniger, F. Druon, E. Mottay, and P. Georges, "Passive coherent combination of two ultrafast rod type fiber chirped pulse amplifiers," *Opt. Lett.* **37**, 1460-1462 (2012).
4. P. Rigaud, V. Kermene, G. Bouwmans, L. Bigot, A. Desfarges-Berthelemot, D. Labat, A. Le Rouge, T. Mansuryan, and A. Barthélémy, "Spatially dispersive amplification in a 12-core fiber and femtosecond pulse synthesis by coherent spectral combining," *Opt. Express* **21**, 13555-13563 (2013).
5. L. P. Ramirez, M. Hanna, G. Bouwmans, H. E. Hamzaoui, M. Bouazaoui, D. Labat, K. Delplace, J. Pouysegur, F. Guichard, P. Rigaud, V. Kermène, A. Desfarges-Berthelemot, A. Barthélémy, F. Prévost, L. Lombard, Y. Zaouter, F. Druon, and P. Georges, "Coherent beam combining with an ultrafast multicore Yb-doped fiber amplifier," *Opt. Express* **23**, 5406-5416 (2015).
6. A. Klenke, M. Müller, H. Stark, F. Stutzki, C. Hupel, T. Schreiber, A. Tünnermann, and J. Limpert, "Coherently combined 16-channel multicore fiber laser system," *Opt. Lett.* **43**, 1519-1522 (2018).
7. M. Müller, A. Klenke, A. Steinkopff, H. Stark, A. Tünnermann, and J. Limpert, "3.5 kW coherently combined ultrafast fiber laser," *Opt. Lett.* **43**, 6037-6040 (2018).
8. S. Jiang, M. Hanna, F. Druon, and P. Georges, "Impact of self-phase modulation on coherently combined fiber chirped-pulse amplifiers," *Opt. Lett.* **35**, 1293-1295 (2010).
9. M. Kienel, A. Klenke, T. Eidam, M. Baumgartl, C. Jauregui, J. Limpert, and A. Tünnermann, "Analysis of passively combined divided-pulse amplification as an energy-scaling concept," *Opt. Express* **21**, 29031-29041 (2013).
10. F. Guichard, L. Lavenu, M. Hanna, Y. Zaouter, and P. Georges, "Coherent combining efficiency in strongly saturated divided-pulse amplification systems," *Opt. Express* **24**, 25329-25336 (2016).
11. Y. Feng, B. M. Zhang, and J. Nilsson, "Photodarkening-induced phase distortions and their effects in single-channel and coherently combined Yb-doped fiber chirped pulse amplification systems," *J. Lightwave Technol.* **36**, 5521-5527 (2018).
12. S. Zhou, F. W. Wise, and D. G. Ouzounov, "Divided-pulse amplification of ultrashort pulses," *Opt. Lett.* **32**, 871-873 (2007).
13. Y. Zaouter, F. Guichard, L. Daniault, M. Hanna, F. Morin, C. Hönniger, E. Mottay, F. Druon, and P. Georges, "Femtosecond fiber chirped- and divided-pulse amplification system," *Opt. Lett.* **38**, 106-108 (2013).
14. T. Zhou, J. Ruppe, C. Zhu, I. Hu, J. Nees, and A. Galvanauskas, "Coherent pulse stacking amplification using low-finesse Gires-Tournois interferometers," *Opt. Express* **23**, 7442-7462 (2015).
15. H. Tünnermann, Y. Feng, J. Neumann, D. Kracht, and P. Weßels, "All-fiber coherent beam combining with phase stabilization via differential pump power control," *Opt. Lett.* **37**, 1202-1204 (2012).
16. H. Lin, Y. Feng, J. H. V. Price, T. W. Hawkins, L. Dong, and J. Nilsson, "Active instantaneous-phase equalization and amplitude control in pulse-bursts in a narrow-linewidth divided-pulse Yb-doped fiber amplification system," in *Laser Congress 2019 (ASSL, LAC, LS&C)*, OSA Technical Digest (Optical Society of America, 2019), paper ATH2A.2.
17. H. Lin, Y. Feng, J. H. V. Price, and J. Nilsson, "Single-shot phase and amplitude fluctuations of narrow-line pulse bursts in divided-pulse amplifier," *IEEE Photonics Technol. Lett.* **31**, 1662-1665 (2019).
18. A. Klenke, M. Wojdyr, M. Müller, M. Kienel, T. Eidam, H. Otto, F. Stutzki, F. Jansen, J. Limpert, and A. Tünnermann, "Large-pitch multicore fiber for coherent combination of ultrashort pulses," in *2015 European Conference on Lasers and Electro-Optics/European Quantum Electronics Conference* (Optical Society of America, 2015), paper CJ_1_2.
19. I. Hartl, A. Marcinkevičius, H. A. McKay, L. Dong, and M. E. Fermann, "Coherent beam combination using multi-core leakage-channel fibers," in *Advanced Solid-State Photonics* (Optical Society of America, 2009), paper TuA6.
20. J. Lhermite, E. Suran, V. Kermene, F. Louradour, A. Desfarges-Berthelemot, and A. Barthélémy, "Coherent combining of 49 laser beams from a multiple core optical fiber by a spatial light modulator," *Opt. Express* **18**, 4783-4789 (2010).
21. J. Noda, K. Okamoto, and Y. Sasaki, "Polarization-maintaining fibers and their applications," *J. Lightwave Technol.* **4**, 1071-1089 (1986).
22. RP Fiber Power v. 7, www.rp-photonics.com/fiberpower.html.
23. H. Dammann and E. Klotz, "Coherent optical generation and inspection of two-dimensional periodic structures," *Opt. Acta* **24**, 505-515 (1977).
24. W. M. Kunkel and J. R. Leger, "Gain dependent self-phasing in a two-core coherently combined fiber laser," *Opt. Express* **26**, 9373 (2018).
25. G. R. Fowles, *Introduction to Modern Optics*, 2nd ed. (Dover Publications, 1989), p. 67.
26. J. R. Leger, "External methods of phase locking and coherent beam addition," in *Surface emitting semiconductor lasers and arrays*, G. Evans and J. Hammer, ed. (Academic Press, 1993), Ch. 8.
27. J. R. Leger, G. J. Swanson, and W. B. Veldkamp, "Coherent laser addition using binary phase gratings," *Appl. Opt.* **26**, 4391-4399 (1987).